Advances in Geo-Energy Research

Vol. 8, No. 3, p. 170-180, 2023

Original article

Effect of drilling and wellbore geometry parameters on wellbore temperature profile: Implications for geothermal production

Mostafa M. Abdelhafiz[1], Joachim Oppelt[2], Omar Mahmoud[1]*, Luiz A. Hegele[3]

[1]*Department of Petroleum Engineering, Future University in Egypt, Cairo 11835, Egypt*

[2]*Drilling Simulator Celle, TU Clausthal, Celle 29221, Germany*

[3]*Department of Petroleum Engineering, Santa Catarina State University, Balneário Camboriú 88336-275, Brazil*

Keywords:
Drilling simulator
wellbore temperature
transient model
geothermal drilling
real-time prediction

Cited as:
Abdelhafiz, M. M., Oppelt, J., Mahmoud, O., Hegele, L. A. Effect of drilling and wellbore geometry parameters on wellbore temperature profile: Implications for geothermal production. Advances in Geo-Energy Research, 2023, 8(3): 170-180.
https://doi.org/10.46690/ager.2023.06.04

Abstract:
Prediction of the wellbore fluids and formation temperatures is crucial during drilling operation, especially for high temperature wells, such as geothermal applications. This work presents the applications of an improved comprehensive drilling simulator for predicting the wellbore system temperature during the drilling process. A fully transient numerical model of the wellbore temperature is developed for drilling and geothermal production applications. The model describes the dynamic behaviour of the thermal state of the wellbore during circulation and static conditions. The developed model is implemented with the commercial virtual drilling simulator through an application programming interface. This implementation allows the coupling of the thermal model with other physical models, which leads to more advanced and realistic simulations. The model has been previously validated through a direct comparison with field data from geothermal well located in the Hanover area in Germany. The results showed a good agreement between the predicted outlet fluid temperature and the measured one. Furthermore, an analysis of the effect of various parameters on the wellbore system temperature is performed. This analysis showed the impact of these parameters on the wellbore temperature profile including the critical areas such as the casing setting point and bottom hole assembly. This information may lead to enhancing the wellbore stability by monitoring the thermal stresses, especially in high-temperature wells. Moreover, predicting the drill bit temperature can result in increasing the lifetime of the bit by adjusting the operating conditions to keep the bit temperature within the specified range. Based on these results, the enhanced drilling simulator with the transient temperature model showed to be a suitable tool for effective well planning.

1. Introduction

Extracting energy from the deep Earth layers is a difficult and complicated procedure. These energy sources are equivalent to renewable geothermal energy or fossil fuels like oil and gas. Additionally, in recent years, energy storage in subsurface formations has become popular. Renewable energy sources like sun and wind are converted into another storable form, such as hot water or hydrogen gas, which is then stored in salt caverns, depleted reservoirs, or underground aquifers.

To be able to create or store this type of energy, it is necessary to drill wells up to thousands of metres deep. There are a number of technical issues with deep wells. Hard formations and high formation temperatures are examples of this, particularly for geothermal purposes. It is difficult to economically drill such type of wells because of these two fundamental issues.

A crucial factor for the proper design of the well is the temperature of the wellbore system. All steps of the

Yandy Scientific Press

*Corresponding author.
E-mail address: mostafa.magdy@fue.edu.eg (M. M. Abdelhafiz); joachim.oppelt@tu-clausthal.de (J. Oppelt); omar.saad@fue.edu.eg (O. Mahmoud); luiz.hegele@udesc.br (L. A. Hegele).

Received May 5, 2023; revised May 21, 2023; accepted June 6, 2023; available online June 10, 2023.

well design can be influenced by the heat transfer process that occurs between the wellbore fluids and the surrounding formation, casing, and cement. These include the properties of the drilling fluid and the cement slurry, and the electrical components used for Measurement While Drilling tool (Fattah et al., 2010; Dirksen, 2011; Zhang et al., 2019; Cayeux, 2020). The rheological characteristics of the drilling fluid are significantly influenced by its temperature. Numerous studies have been conducted to simulate how temperatures affect the characteristics of drilling fluids (Annis, 1967; Wang et al., 2012; Vryzas et al., 2017; Ohenhen et al., 2018). They have concluded that the temperature directly affects the density, gel strength, yield point, and viscosity of drilling fluid. The drilling process may be impacted by changes to these variables. The drilling fluid's insufficient viscosity might cause serious issues with wellbore cleaning (Gautam and Guria, 2020). The annular pressure losses are also impacted by viscosity, which affects the equivalent circulating density value (Ataga and Ogbonna, 2012). This value is critical and especially during drilling wells with narrow mud windows, which is the margin between the pore pressure and the fracture pressure.

Moreover, Zhang et al. (2019) performed a study on the influence of the temperature changes on wellbore stability. They have determined that during the thermal recovery periods where the circulation stopes and the wellbore fluid remain static, the wellbore walls can experience severe damage. This occurs due to the effect of temperature on the mechanical properties of the rock.

Additionally, other researchers such as Choi and Tan (1998), Chen and Ewy (2005), and AlBahrani et al. (2018) have considered time-dependent wellbore stability issues resulting from the drilling fluid temperature variations. They have concluded in their work that the temperature difference inside the wellbore can result in a reduction of the rock grains volume in the wellbore wall, which may reduce the hoop stresses. This phenomenon depends highly on the thermal behaviour and the physical properties of the rock including the thermal expansion coefficient and the porosity. Additional critical aspect regarding the thermal effects on the wellbore stability occurs during drilling gas hydrate reservoirs. Li et al. (2019) explored the thermal effect on the wellbore wall integrity in gas hydrate reservoirs. They have concluded a relationship between the drilling fluid temperature and the borehole collapse.

Beside the wellbore stability issue, the temperature of the wellbore can affect different parameters during cement slurry design. Different researchers have noted the direct effect of the temperature on cement properties such as, thickening time, compressive strength, and the rheology of the cement during cementing operation (Pernites et al., 2017). Moreover, the temperature has a direct impact on the main chemical reactions that control the hydration of the cement slurry. Overestimating or underestimating the wellbore temperature will result in a variety of non-productive time events, ranging from excessive Wait on Cement to drilling-out of cementing of the casing (Chen and Novotny, 2003).

All that have been said shows the importance of accurate modelling and simulation of the borehole temperature and the surrounding formation during drilling. Precise prediction and simulation of those temperatures should be supported by a comprehensive dynamic study of the heat transfer between the wellbore fluid and the surrounding formation.

In the last decades, various studies have been performed to investigate the influence of temperature on the wellbore system. This includes different studies during oil and gas production operation (Hasan and Kabir, 1996; Hasan et al., 2005; Onur and Cinar, 2017), and during steam injection operation (Almeida and Rahnema, 2017), and during the drilling operation (Santoyo et al., 2003; Xu et al., 2018). Xu et al. (2018) studied the effect of a gas kick on the temperature distribution of the wellbore. Santoyo et al. (2003) were concerned about the loss of circulation problem and its effect on the temperature profile. Moreover, different research modelled the effect of the shut-in operation on the thermal response on the wellbore system (García et al., 1998a, 1998b; Santoyo et al., 2003; Abdelhafiz et al., 2021). Additionally, various research work investigated the effect of the fluid properties on the wellbore temperature. Zhang et al. (2021) have presented a work investigating the effect of various thermophysical properties of the drilling fluids on the wellbore system temperature. These parameters include the density, thermal conductivity, specific heat capacity, and viscosity of drilling fluid. According to their results, the changes in density and thermal conductivity of drilling fluid due to temperature have a minimal impact on the calculation of wellbore temperature. Similarly, the effect of the drilling fluid's specific heat capacity variation with temperature on wellbore temperature calculation is negligible. However, the viscosity variation of the drilling fluid with temperature has a significant impact on the calculation of wellbore temperature.

To the best of authors' knowledge, the effect of various drilling parameters on the temperature of the wellbore is not studied. These parameters include the rate of penetration (ROP) and the heat generated at the bit/rock interface. Additionally, previous models consider a constant inlet fluid temperature, however, the effect of this assumption is still not well known.

Therefore, in this paper, a thermal analysis of the wellbore system is conducted to investigate the effect of the aforementioned parameters on the wellbore temperature profile during the drilling operation. For this objective, an improved virtual drilling simulator is utilized. This paper is structured as follows; after the introduction, the methodology of this work is presented, where the thermal model of the wellbore system is described. Additionally, the main components of the virtual drilling simulator are also elaborated. Then, the application of the model in a simulation case and the results of the analysis using the developed model are also presented and thoroughly discussed. Finally, the conclusions of the work are summarized.

2. Methodology

The approach proposed by this work is to perform and analyse the wellbore system temperature using physics virtual

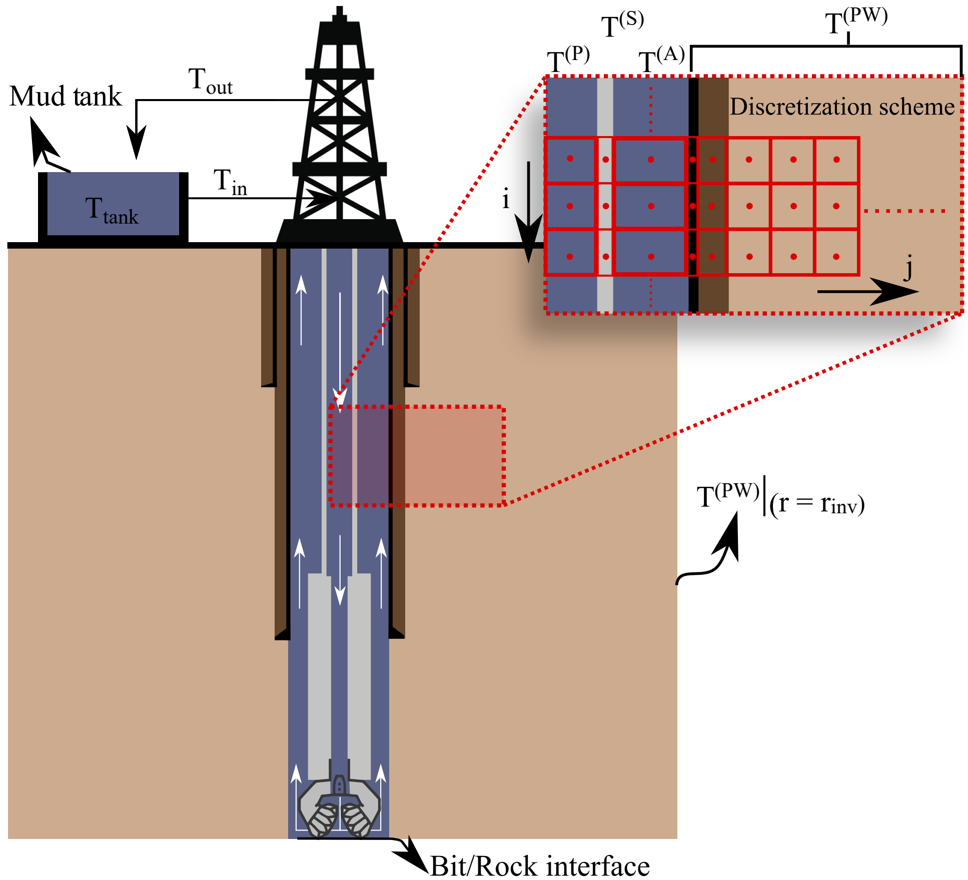

Fig. 1. Basic wellbore sketch representing the main components of the thermal model and the discretization scheme.

simulator for realistic drilling scenarios. This approach has been followed by different authors for training purposes and for drilling cost optimization (Scott et al., 2016; Tang et al., 2016; Höhn et al., 2019). In this section, a mathematical model that describes the thermal behaviour of the wellbore during drilling operation is illustrated. The model is implemented in a comprehensive virtual drilling simulator to calculate the temperature variation in the wellbore components during a realistic drilling scenario.

2.1 Modeling the wellbore temperature

The first step in modelling the thermal behaviour of the wellbore is to identify the basic component of the system. Fig. 1 presents a generalized wellbore sketch with the basic components during the drilling operation. As per our previous work in Abdelhafiz et al. (2021), the wellbore system is divided into two main regions. the first region is the wellbore, and the second region the post wellbore.

In the first region, which represents the wellbore itself, we focus on the fluid inside the drillstring, the drill string walls, and the fluid within the annulus between the wellbore walls and the drill string. This section is treated as a one dimensional in space along the axial direction, allowing us to analyse temperature changes over time and along the length of the wellbore. By considering the axial dimension, we can account for variations in temperature along the wellbore depth and effectively model heat transfer processes in the drilling fluid and drill string. The heat transfer in the radial direction in this region is accounted through three different convective heat transfer coefficients. This allows for accurately describe the phenomenon within each flowing section.

The second section, known as the post-wellbore section, encompasses the rock formation, casing, and cement. In this section, we introduce a two-dimensional space that includes both the axial and radial dimensions, in addition to the time dimension. This enables us to accurately represent the radial temperature distribution within the surrounding rock formation and the thermal interactions between the casing, cement, and the wellbore. By incorporating the radial dimension, we can better capture the effects of heat conduction in the post-wellbore environment.

To couple these two regions, the balance equation at the wellbore walls is solved. This ensures that energy is exchanged appropriately between the wellbore and the post-wellbore sections, allowing for a more accurate representation of the overall thermal behaviour of the wellbore system.

The model further assumes the decoupling of the energy and momentum equations, which limits its applicability to incompressible fluids. Additionally, all thermophysical properties are considered independent of temperature. These assumptions greatly simplify the model and reduce computational requirements, making it faster to run. Moreover, these assumptions align well with the specific application of the model as the drilling fluid can be assumed as incompressible fluids.

2.2 Governing equation

For each of the described regions above, a thermal balance equation is developed that describes the heat transfer within and between the different zones. The complete set of equations is published in Abdelhafiz et al. (2021), and Abdelhafiz (2022), and it is repeated here for the sake of clarity:

$$\frac{\partial(\rho_f c_{p,f} T^{(P)})}{\partial t} + \frac{\partial(\rho_f c_{p,f} T^{(P)} u_{z,P})}{\partial z} = -\frac{2h_P k_s (T^{(P)} - T^{(S)})}{r_{P,in}\left(k_s + h_p r_{P,in} \ln \frac{r_s^*}{r_{P,in}}\right)} \tag{1}$$

$$\frac{\partial\left(\rho_s c_{p,s} T^{(S)}\right)}{\partial t} = -\frac{2h_p k_s \left(T^{(S)} - T^{(P)}\right)}{r_{P,in}\left(k_s + h_p r_{P,in} \ln \frac{r_s^*}{r_{P,in}}\right)} - \frac{2h_{A,in} k_s r_{P,out}\left(T^{(S)} - T^{(A)}\right)}{\left(r_A^2 - r_{P,out}^2\right)\left(k_s + h_{A,in} r_{P,out} \ln \frac{r_{P,out}}{r_s^*}\right)} \tag{2}$$

$$\frac{\partial\left(\rho_f c_{p,f} T^{(A)}\right)}{\partial t} + \frac{\partial\left(\rho_f c_{p,f} T^{(A)} u_{z,A}\right)}{\partial z} = -\frac{2h_{A,in} k_{P,out}\left(T^{(A)} - T^{(S)}\right)}{\left(r_A^2 - r_{P,out}^2\right)\left(k_S + h_{A,in} r_{P,out} \ln \frac{r_{P,out}}{r_S^*}\right)} - \frac{2h_{A,out} r_A\left(T^{(A)} - T^{(PW)}\right)}{\left(r_A^2 - r_{P,out}^2\right)\left(k + h_{A,out} r_A \ln \frac{r_{j=1}^*}{r_A}\right)} \tag{3}$$

$$\frac{\partial\left(\rho c_p T^{(PW)}\right)}{\partial t} = \frac{\partial}{\partial z}\left(k \frac{\partial T^{(PW)}}{\partial z}\right) + \frac{1}{r}\frac{\partial}{\partial r}\left(rk \frac{\partial T^{(PW)}}{\partial r}\right) \tag{4}$$

where Eqs. (1)-(4) account for the temperature of the fluid flowing inside the drill string $T^{(P)}$, °C; the drill string $T^{(S)}$, °C; the fluid flowing inside the annulus $T^{(A)}$, °C; and finally, the formation casing and cement $T^{(PW)}$, °C. t is the time, s; and z accounts for the vertical coordinate, m; and r is for the radial coordinate, m. The equations account for the radial heat transfer using three different convective heat transfer coefficients. h_P is the convection heat coefficient for the flow in the drill string, W/m^2·K; $h_{A,in}$ and $h_{A,out}$ are the convection heat coefficient for the flow in the inner and the outer annulus respectively, W/m^2·K. $r_{P,in}$ and $r_{P,out}$ are the inner and the outer radius of the drill string respectively, m; while r_A annulus radius, m. r_s^* is the local radius, m; in the drill string section having the mean temperature, which can be assumed to be equal to $(r_{P,in} + r_{P,out})/2$. ρ, kg/m^3; c_p, J/kg·K; and k, W/m·K; are the density, the specific heat, and the thermal conductivity index with the subscripts f and s which denote the fluid and the drill string solid sections, respectively. $u_{z,P}$ and $u_{z,A}$ are the fluid flowing velocities in the drill string and the annulus, respectively, m/s. $r_{j=1}^*$, m; is the local radius of the first grid in the radial direction of the post wellbore zone where the average cell temperature is located, here it is assumed to be the cell centre. The previous set of equations is solved numerically using the finite volume method with the upwind scheme (Abdelhafiz et al., 2020).

The model described in Eqs. (1)-(4) shows that it is physics-based model which can be applied for various geological formations and drilling conditions. The model discretizes the formation and wellbore properties and solves the thermal balance equation, offers flexibility in accommodating diverse geological properties. The discretization of the formation and wellbore into a number of cells with finite volumes allows our model to capture the spatial variations in thermophysical properties. This feature enables the consideration of different geological formations with varying characteristics such as rock type, density, specific heat capacity, and thermal conductivity. By assigning the appropriate thermophysical properties to each cell, the model accurately represents the complexities of the subsurface system.

To ensure the reliability and applicability of our model across various regions, we have undertaken rigorous validation efforts. The numerical solution has been validated using theoretical methods, computational methods and employing a comparison with the field and experimental data obtained from geothermal wells in Mexico, Norway, and Sweden (Abdelhafiz et al., 2023). The comparisons have consistently demonstrated good agreement between our model predictions and the observed data (Abdelhafiz, 2022).

2.3 Initial and boundary conditions

The model is initiated with a temperature equivalent to the initial geothermal temperature: The initial conditions for the temperature for both models are assumed equal to the geothermal temperature. Therefore, at time $t = 0$:

$$T^{(P)}(z,t=0) = T^{(S)}(z,t=0) = T^{(A)}(z,t=0) = T^{(PW)}(r,z,t=0) = T_e + \left.\frac{\Delta T}{\Delta z}\right|_e (z-L) \tag{5}$$

where T_e is the surface ambient temperature, °C; and $(\Delta T/\Delta z)|_e$ is the geothermal gradient, °C/m; and L is the well total length, m. For the boundary conditions, the following is applied to the bottom of the wellbore:

$$T^{(A)}\big|_{(i=1)} = T^{(P)}\big|_{(i=1)} \tag{6}$$

where the subscript $(i=1)$ donates the first cell at the wellbore bottom in the discretised scheme according to Fig. 1. The additional heat generated at the interface between the drill bit and the rock formation due to friction is added according to Glowka and Stone (1985):

$$Q_f = \frac{K_f F_N v}{A_c} \tag{7}$$

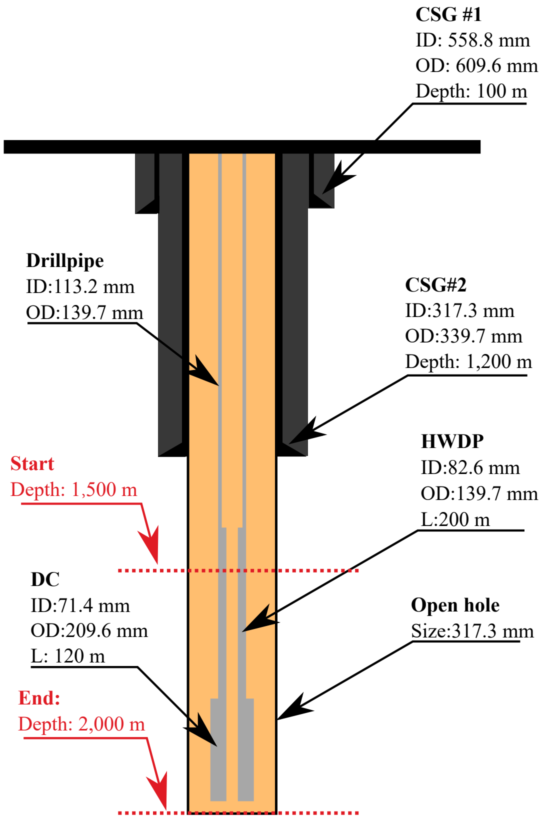

Fig. 2. Wellbore sketch of the proposed well for the study.

where Q_f, W/m^2; is the heat rate generated due to friction per bit/rock contact area, K_f is the coefficient of friction between the bit cutters and the formation, F_N, N; and v, m/s; are the normal force acting in the drill bit and the drill bit speed, respectively. The normal force is considered as the weight on bit (WOB), and the bit speed is derived from the bit rotational speed (RPM). A_c is the contact surface area between the drill bit and the formation in m^2.

While at the surface: the boundary conditions for the drill pipe, drill pipe walls, and the annulus vary between flowing and shut-in conditions. In addition to the first grid volume in the post-wellbore section (i.e., $j = 1$). For the flowing conditions, the following boundary conditions are applied:

$$T^{(P)}\big|_{(i=N_v)} = T_{in} \tag{8}$$

where T_{in} is the inlet fluid temperature in °C and calculated by performing energy balance on the mud tank:

$$\begin{aligned} m_{tank} c_{p,f} (T_{tank} - T^0_{tank}) = \\ \dot{m}_{in} c_{p,f} (T^{(A)}_{out} - T^{(P)}_{in}) \Delta t - \dot{Q}_{\text{loss}} \Delta t \end{aligned} \tag{9}$$

where T_{tank} is the final tank temperature, °C; T^0_{tank} is the initial tank temperature, °C; $T^{(A)}_{out}$ and $T^{(P)}_{in}$ are the drilling fluid outlet temperature from the wellbore and inlet temperature to the wellbore respectively in °C. m_{tank} is the fluid mass inside the tank, kg; $\dot{m}_{in}$ is the mass flow rate of the return fluid, kg/s; and finally, Δt is the time step, s; $\dot{Q}_{\text{loss}}$ is the heat rate loss/gain to the ambient surface air due to free convection, W.

2.4 The virtual drilling simulator

The German Centre for High-Performance Drilling and Automation which is known as Drilling Simulator Celle is recently equipped with the state-of-the-art virtual drilling simulator. This simulator is utilized for training and for research and development applications (Höhn et al., 2019).

The simulator's capabilities extend beyond its initial configuration, due to the availability of an Application Programming Interface (API). This API enables the incorporation of newly developed downhole models, which can be seamlessly connected to the simulator's internal models. By utilizing the API, the simulator can be constantly improved and customized according to specific requirements. The potential applications of integrating physical modelling into the virtual drilling simulator are vast. For instance, it can facilitate the development and testing of advanced drilling systems, such as automated drilling rigs or autonomous drilling operations. By incorporating physical models into the simulator, researchers can assess the feasibility and performance of such systems before deploying them in real-world scenarios. Additionally, the simulator can be utilized to study the behaviour of different drilling fluids, wellbore stability, and the effects of various drilling techniques on the surrounding formations.

Furthermore, the virtual drilling simulator serves as a valuable research and development tool. It enables engineers and researchers to explore and experiment with different downhole models, evaluating their performance, efficiency, and impact on drilling operations. The simulator allows for testing and validation of innovative drilling technologies, equipment designs, and drilling techniques. By integrating physical modelling, researchers can analyse complex interactions between drilling parameters, downhole conditions, and the resulting drilling performance. This information can be used to optimize drilling processes, enhance equipment reliability, and minimize drilling risks.

Moreover, the simulator's API allows for seamless communication between the simulator and the external physical models. This integration opens up possibilities for real-time monitoring and control of drilling parameters. For instance, a physical thermal model can be linked with the simulator to provide accurate temperature predictions in the downhole environment. This information can then be utilized for operational decision-making, optimizing drilling parameters, and ensuring wellbore integrity.

In order to dynamically simulate the transient thermal behaviour of the wellbore, a computer code has been developed based on the thermal model described in Section 2. The code has been implemented in two versions, utilizing MATLAB® and C# programming languages. The MATLAB® version serves as a stand-alone thermal simulator, allowing users to execute simulations independently. The authors have made the MATLAB® code available online (Abdelhafiz, 2021), enabling researchers to access and utilize it for their own investigations. On the other hand, the C# version of the code is integrated with the virtual drilling simulator mentioned earlier, leveraging an API for seamless interaction. This integration facilitates a comprehensive analysis of the thermal aspects within the con-

Table 1. Drill string and drilling fluid properties.

Property	Rock formation	Drill string	Casing	Cement	Drilling fluid
ρ (kg/m^3)	1,800	8,000	7,800	2,140	1,220
c_p (J/kg·K)	1,250	440	420	2,000	1,600
k (W/m·K)	2.5	47.7	47.2	1.1	1.2
μ (Pa·s)	-	-	-	-	0.025

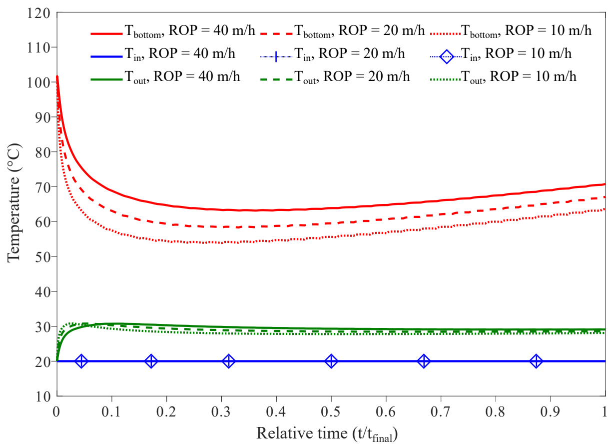

Fig. 3. Inlet, outlet, and bottom hole temperatures for rate of penetration 40, 20 and 10 m/h using constant inlet temperature.

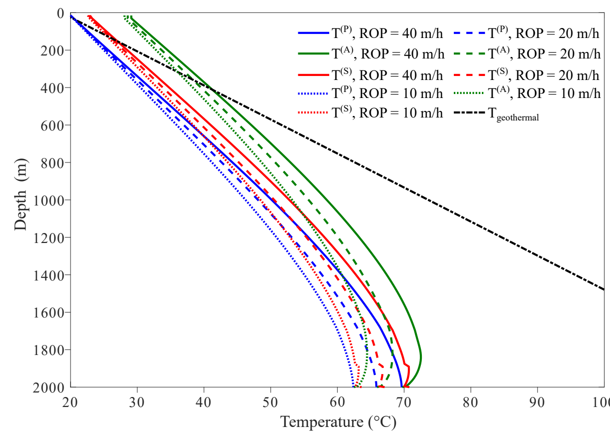

Fig. 4. Final temperature profile of the wellbore for rate of penetration 40, 20 and 10 m/h using constant inlet temperature.

text of the virtual drilling environment.

3. Results and discussion

3.1 Case setup

To perform the thermal analysis, a drilling scenario case was set up. Fig. 2 shows a sketch of the wellbore that is utilized for this study. The figure represents the main wellbore system and downhole components. The case includes a complex drill string from three parts and two installed casing strings as shown in the figure. The simulations start at an initial depth of 1,500 m, and end when the drill-bit reaches the depth of 2,000 m. The thermophysical properties of the rock formation, drilling fluid, drill strings, casing strings and cement are summarized in Table 1.

In this simulation, the domain is discretized spatially into 100 grid cells in the vertical direction and 20 cells in the radial direction. This allows for a comprehensive representation of the physical space under consideration. To ensure stability and accuracy in the temporal discretization, the time step is selected such that the Courant number, remains below 1. In this case, a Courant number of 0.8 is chosen, striking a balance between solution stability and computational efficiency. The time step is calculated according to the following equation:

$$\Delta t = \frac{0.8\Delta z}{u_{z,P}} \tag{10}$$

This approach maximizes the stability of the numerical solution while maintaining a reasonable level of temporal resolution. For each simulation case, the initial and boundary conditions are established based on Eqs. (6)-(9), as outlined in Section 2.2.

3.2 Effect of ROP on the wellbore system temperature

The first comparison case was developed to analyse the effect of the ROP on the thermal behaviour of the wellbore. To that extent, two simulation packages were performed. Each simulation package has three simulation runs with rate of penetration values of 10, 20, and 40 m/h. The first simulation package assumes a constant inlet fluid temperature T_{in} is const. The results can be summarized in Figs. 3 and 4.

In Fig. 4, the inlet, outlet and the bottom hole temperature are recorded with relative time t/tfinal, where tfinal is the final simulation time. The inlet temperature for this simulation case was kept constant, which can be observed in Fig. 3 as the inlet temperature curve for the three simulation cases are overlayed with value of 20 °C. It is clearly shown that the ROP has a direct effect on the bottom hole temperature. A difference of 7 °C is observed between the 40 and 20 m/h cases after reaching the final depth. Regarding the outlet temperature, no significant effect is observed. The vertical temperature profiles presented in Fig. 4 show that the effect is major deep in the wellbore, however, it decreases towards the surface.

The second simulation package on the effect of the ROP on the wellbore thermal behaviour is performed with calculated inlet fluid temperature. T_{in} is assumed to be equal to the mud tank temperature $T_{in} = T_{tank}$ which is calculated according to Eq. (9). The results from these simulations are summarized in Figs. 5 and 6.

In comparison with the previous case (constant inlet tem-

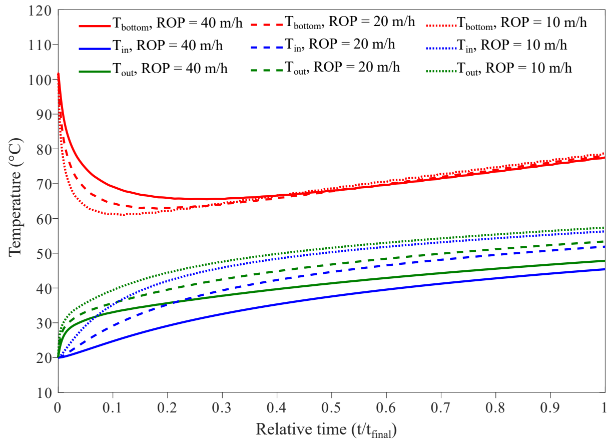

Fig. 5. Inlet, outlet, and bottom hole temperatures for rate of penetration 40, 20 and 10 m/h using calculated inlet temperature.

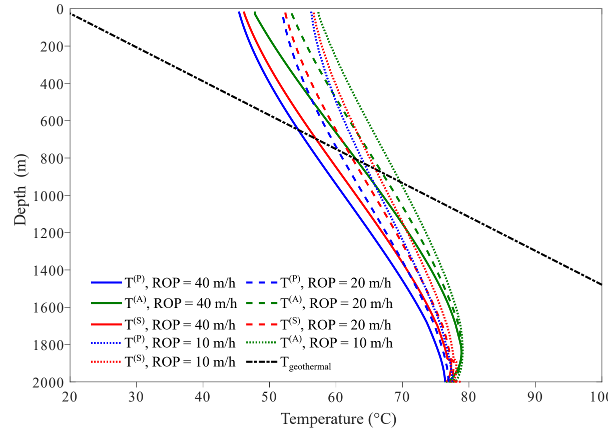

Fig. 6. Final temperature profile of the wellbore for rate of penetration 40, 20 and 10 m/h using calculated inlet temperature.

perature), A major difference can be observed. For the calculated inlet temperature case, the ROP shows initially an observable effect on the bottom hole temperature, however, after the circulation of bottoms up, the difference in the bottom hole temperature with respect to the ROP is negligible. On the other hand, a major effect is observed on the inlet and the outlet temperatures. The ROP shows an inverted effect on those temperatures, as the low ROP values show the highest inlet and outlet temperature.

3.3 Effect of the heat generated due to bit/rock interaction on the wellbore system temperature

The second set of simulations is aiming to analyse the effect of the heat generated due to friction between the bit and the formation during drilling. The parameters that control this effect which are the WOB, bit RPM, and K_f are analysed in case of low circulation rate and high circulation rate. During drilling, WOB and RPM varies according to the drilling program which are optimized for the highest ROP values. However, K_f depends on the rock formation type and the drill bit. For example, rough and abrasive formations may have higher K_f than soft formations. Additionally, one important factor that may affect the friction between the formation and the bit is the bit wear. As the bit wears down, the friction coefficient can change, affecting the heat generation process. This alteration in heat generation can subsequently influence the temperature profile within the wellbore. The results which are presented in Figs. 7-9 show a minor effect of the previously mentioned parameter on the bottom hole temperature in case of low circulation rate, and almost no effect is observed at the inlet and the outlet temperature. In case of a high circulation rate, a slight increase in the bottom hole temperature for higher values of K_f , WOB and RPM, however, no observed effect on the inlet and the outlet temperature.

3.4 Effect of the drilling and abnormal formation on the wellbore system temperature

The next simulation is designed to analyse the effect of drilling an abnormal formation on the wellbore system temperature. In this work, the term abnormal is used for a formation that has extremely different thermal properties than its overburden and sub-burden formation. This situation can be found in different geological structures. For example, sand lenses that are submerged in shale formations, or magmatic dikes. This can cause an abrupt change in the physical and the thermal properties of the formation. For that reason, a simulation case was set up by creating an anomaly in the formation thermophysical properties within a specific formation thickness as described by Fig. 10. The formation properties -which are ρ, c_p and k - within this abnormal formation are considered to have double the magnitude of the overburden and the sub-burden formation. The resultant effect on the temperature behaviour is plotted with respect to time in Fig. 11.

Fig. 11 shows a comparison between the inlet, outlet, and the bottom hole temperatures in case of normal formation without anomalies (curves marked with O) and of the formation which include an anomaly at depth 1,600 m and a thickness of 260 m (curves marked with $+$). The plot also indicates the relative time which the abnormal formation has been penetrated, which in this case at relative time is 0.2. From the plot, one can observe an instantaneous change in the bottom hole temperature once reaching the abnormal formation. The temperature increase in the bottom hole reaches up to 10 °C. The rate of change in the bottom hole temperature is decreased once passing the abnormal formation, which is indicated on the graph by the dashed vertical line at relative time is 0.72.

On the other hand, a slightly delayed effect on the outlet fluid temperature is also observed after reaching the abnormal formation. This delay is due to the lag time between the bottom hole and the surface. This delay will be function of the well depth and the annular fluid velocity. The magnitude of the change in the outlet temperature should be dependent on the formation properties.

This result shows the significance of interpreting the bottom hole temperature and the outlet temperature to get information about the downhole formation.

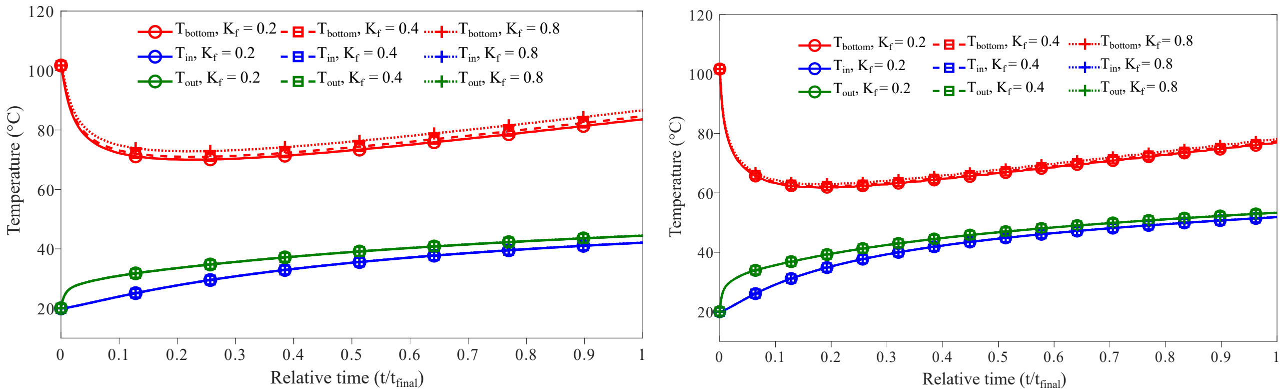

(a) (b)

Fig. 7. Effect of the K_f between the drill-bit and the formation on the bottom-hole, inlet, and outlet temperatures in case of (a) low circulation rate case $\mathrm{Q} = 54\,\mathrm{m}^3/\mathrm{h}$ and (b) high circulation rate case $\mathrm{Q} = 108\,\mathrm{m}^3/\mathrm{h}$.

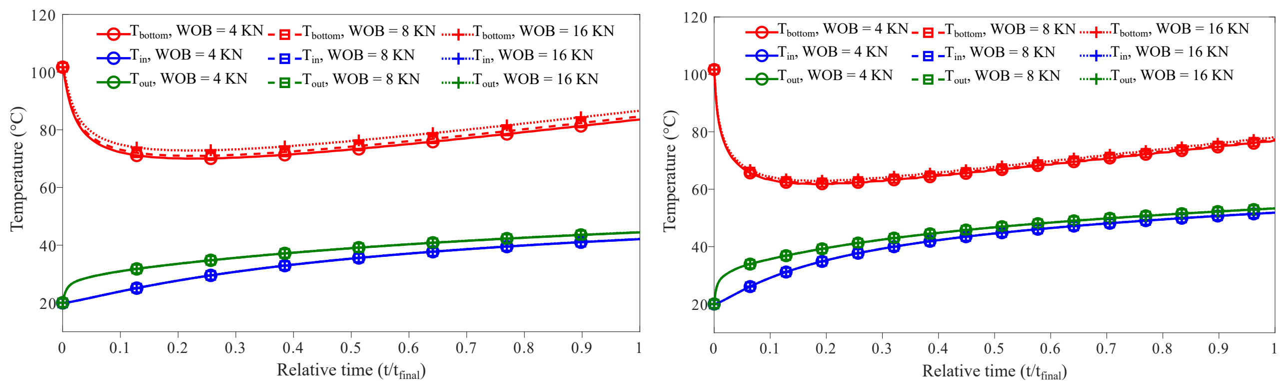

(a) (b)

Fig. 8. Effect of the WOB on the bottom-hole, inlet, and outlet temperatures in case of (a) low circulation flow rate case $\mathrm{Q} = 54\,\mathrm{m}^3/\mathrm{h}$ and (b) high circulation flow rate case $\mathrm{Q} = 108\,\mathrm{m}^3/\mathrm{h}$.

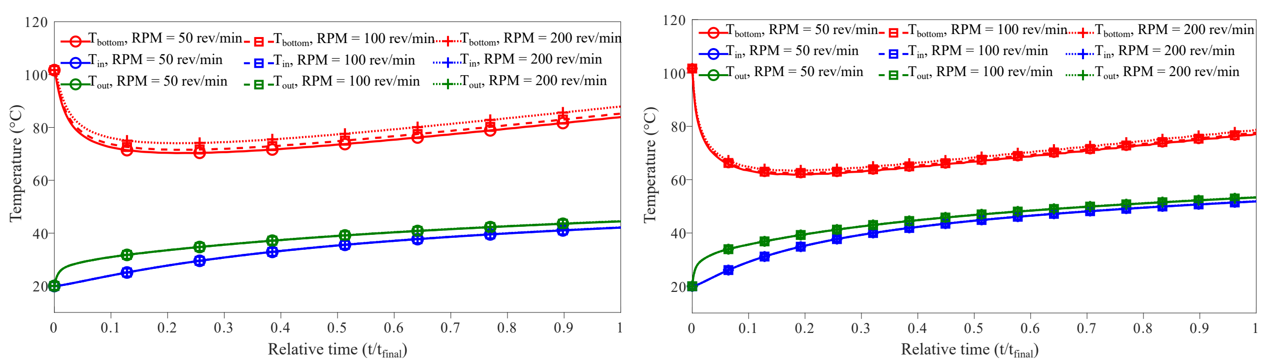

(a) (b)

Fig. 9. Effect of the bit RPM on the bottom-hole, inlet, and outlet temperatures in case of (a) low circulation flow rate case $\mathrm{Q} = 54\,\mathrm{m}^3/\mathrm{h}$ and (b) high circulation flow rate case $\mathrm{Q} = 108\,\mathrm{m}^3/\mathrm{h}$.

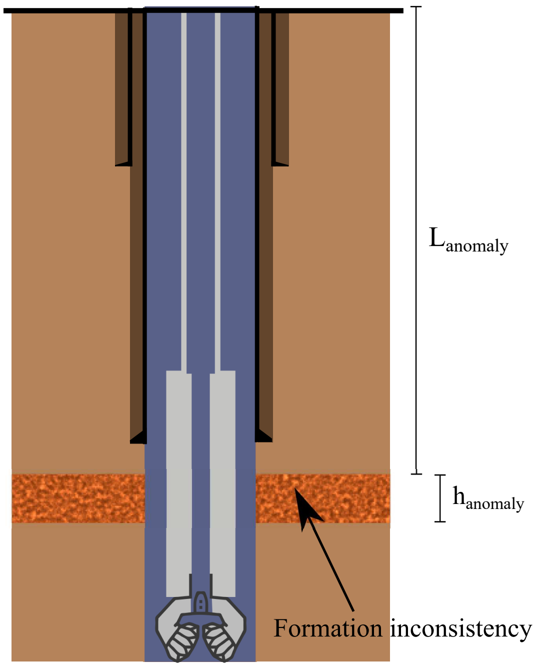

Fig. 10. Sketch representing an inconsistent formation with abnormal properties encountered during drilling.

4. Conclusions

In this paper, a thermal analysis was conducted on the wellbore system during drilling using an improved drilling simulator. The study focused on examining the impact of drilling parameters on the inlet and outlet drilling fluid temperatures. The findings of the analysis provide several important insights.

Firstly, the rate of penetration was found to exert a significant influence on the temperature of the wellbore system. This highlights the importance of considering the drilling speed when assessing thermal behaviour. Secondly, it was observed that assuming a constant inlet fluid temperature greatly affected the wellbore's thermal performance. This emphasizes the need to accurately account for temperature variations in the inlet fluid. While the WOB and RPM had a minor effect on the drilling fluid's temperature at low flow rates, their impact became negligible at high-volume flow rates. This suggests that WOB and RPM have limited significance in terms of temperature variation unless the drilling fluid flow rate is substantial. The simulation results also revealed the high sensitivity of the wellbore system's temperature to the properties of the formation being drilled. This underscores the importance of considering formation properties when predicting the thermal behaviour of the wellbore.

Additionally, the bottom hole temperature was found to be highly sensitive to changes in formation properties, whereas the outlet fluid temperature displayed less responsiveness to variations in subsurface thermal properties. These findings demonstrate the potential of accurate modelling and simulation in enhancing drilling efficiency. By predicting the thermal behaviour of the wellbore under different conditions, issues related to drilling fluid properties and bit lifespan can be mitigated. Furthermore, maintaining a consistent inlet temperature of the drilling fluid using sufficiently large mud tanks during circulation can significantly reduce the overall temperature profile of the wellbore. This highlights the practical importance of temperature control during the drilling operation.

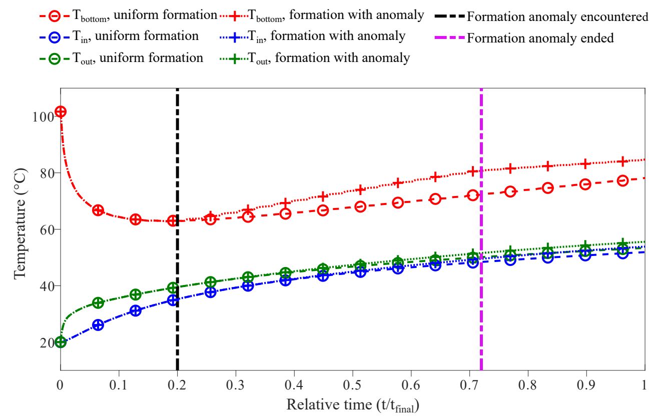

Fig. 11. Effect of an abnormal formation layer at depth $L_{anom} = 1,600$ m and thickness $h_{anom} = 260$ m on the bottom-hole, inlet, and outlet temperature.

Acknowledgements

The authors would like to thank Prof. Dr. Philip Jaeger for a critical reading of the manuscript and insightful suggestions. The authors would like to express appreciation for the Future University in Egypt and the faculty members in the department of petroleum engineering for their continuous encouragement and support.

Conflict of interest

The authors declare no competing interest.

References

Abdelhafiz, M. M. Wellbore Temperature Simulator. 2021.

Abdelhafiz, M. M. Modelling and simulating the thermal interaction between the wellbore fluids and rock formation during drilling operations. Clausthal-Zellerfeld, Clausthal University of Technology, 2022.

Abdelhafiz, M. M., Hegele Jr, L. A., Oppelt, J. F. Numerical transient and steady state analytical modelling of the wellbore temperature during drilling fluid circulation. Journal of Petroleum Science and Engineering, 2020, 186: 106775.

Abdelhafiz, M. M., Hegele Jr, L. A., Oppelt, J. F. Temperature modeling for wellbore circulation and shut-in with application in vertical geothermal wells. Journal of Petroleum Science and Engineering, 2021, 204: 108660.

Abdelhafiz, M. M., Oppelt, J. F., Brenner, G., et al. Application of a thermal transient subsurface model to a coaxial borehole heat exchanger system. Geoenergy Science and Engineering, 2023, 227: 211815.

AlBahrani, H. I., Al-Qahtani, A., Hamid, O., et al. An investigation of the relationship between the time-dependent wellbore stability and the related operational practices. Paper OTC 28285 Presented at the Offshore Technology Conference Asia, Kuala Lumpur, Malaysia, 20-23 March, 2018.

Almeida, R. V., Rahnema, H. Multiphase thermal compositional wellbore modeling in hybrid steam/solvent injection. Paper SPE 182668 Presented at the SPE Reservoir Simulation Conference, Montgomery, Texas, 20-22 February, 2017.

Annis, M. R. High-temperature flow properties of water-base drilling fluids. Journal of Petroleum Technology, 1967, 19(8): 1074-1080.

Ataga, E., Ogbonna, J. Accurate estimation of equivalent circulating density during high pressure high temperature (HPHT) drilling operations. Paper SPE 162972 Presented at the Nigeria Annual International Conference and Exhibition, Lagos, Nigeria, 6-8 August, 2012.

Cayeux, E. Time, pressure and temperature dependent rheological properties of drilling fluids and their automatic measurements. Paper SPE 199641 Presented at the IADC/SPE International Drilling Conference and Exhibition, Galveston, Texas, 3-5 March, 2020.

Chen, G., Ewy, R. T. Thermoporoelastic effect on wellbore stability. SPE Journal, 2005, 10 (2): 121-129.

Chen, Z., Novotny, R. J. Accurate prediction wellbore transient temperature profile under multiple temperature gradients: Finite difference approach and case history. Paper SPE 84583 Presented at the SPE Annual Technical Conference and Exhibition, Denver, Colorado, 5-8 October, 2003.

Choi, S. K., Tan, C. P. Modelling of effects of drilling fluid temperature on wellbore stability. Paper SPE 47304 Presented at the SPE/ISRM Rock Mechanics in Petroleum Engineering, Trondheim, Norway, 8-10 July, 1998.

Dirksen, R. Upgrading formation-evaluation electronics for high-temperature drilling environments. Journal of Petroleum Technology, 2011, 63(1): 24-26.

Fattah, K. A., El-Katatney, S. M., Dahab, A. A. Potential implementation of underbalanced drilling technique in Egyptian oil fields. Paper SPE 130711 Presented at the International Oil and Gas Conference and Exhibition in China, Beijing, China, 8-10 June, 2010.

García, A., Hernandez, I., Espinosa G. et al. TEMLOPI: A thermal simulator for estimation of drilling mud and formation temperatures during drilling of geothermal wells. Computers & Geosciences, 1998a, 24(5): 465-477.

García, A., Santoyo, E., Espinosa, G. et al. Estimation of temperatures in geothermal wells during circulation and shut-in in the presence of lost circulation. Transport in Porous Media, 1998b, 33: 103-127.

Gautam, S., Guria, C. Optimal synthesis, characterization, and performance evaluation of high-pressure high-temperature polymer-based drilling fluid: The effect of viscoelasticity on cutting transport, filtration loss, and lubricity. SPE Journal, 2020, 25(3): 1333-1350.

Glowka, D. A., Stone, C. M. Thermal response of polycrystalline diamond compact cutters under simulated downhole conditions. SPE Journal, 1985, 25(2): 143-156.

Hasan, A. R., Kabir, C. S. A mechanistic model for computing fluid temperature profiles in gas-lift wells. SPE Production and Facilities, 1996, 11(3): 179-185.

Hasan, A. R., Kabir, C. S., Lin, D. Analytic wellbore temperature model for transient gas-well testing, SPE Reservoir Evaluation & Engineering, 2005, 8(3): 240-247.

Höhn, P., Freifer, R., Oppelt, J. Realistic scenario drilling simulation for deep and critical wells. Paper OMC 2019-1187 Presented at the Offshore Mediterranean Conference and Exhibition, Ravenna, Italy, 27-29 March, 2019.

Li, Q., Cheng, Y., Wang, G. et al. Determination of safe mud temperature window for drilling operation in hydrate deposits in Shenhu Area, Northern South China Sea. Paper ISOPE I 19-664 presented at the 29th International Ocean and Polar Engineering Conference, Honolulu, Hawaii, 16-21 June, 2019.

Ohenhen, I., Ogiriki, S. O., Imuetiyan, I. et al. Experimental study of temperature effect on drilling mud with local additives. International Journal of Engineering Research in Africa, 2018, 38: 9-16.

Onur, M., Cinar, M. Modeling and analysis of temperature transient sandface and wellbore temperature data from variable rate well test data. Paper SPE 185802 Presented at the SPE Europec featured at 79th EAGE Conference and Exhibition, Paris, France, 12-15 June, 2017.

Pernites, R., Clark, J., Santra, A. New polymeric high temperature cement retarder with synergistic suspending aid property in fluid loss control polymers. Paper SPE 184556 presented at the SPE International Conference on Oilfield Chemistry, Montgomery, Texas, 3-5 April 2017.

Santoyo, E., Garcia, A., Espinosa, G., et al. Convective heat-transfer coefficients of non-Newtonian geothermal drilling fluids. Journal of Geochemical Exploration, 2003, 78: 249-255.

Scott, L., Wessel, J. S., Nabavi, J., et al. Use of a life cycle drilling simulation system on a challenging HPHT drilling operation in the Norwegian Sea. Paper SPE 178207 Presented at the SPE/IADC Middle East Drilling Technology Conference and Exhibition, Abu Dhabi, UAE, 26-28 January, 2016.

Tang, H. Y., Gang, W., Rommetveit, R. et al. Advanced drilling simulation and engineering centre provide support for challenging drilling operations in the South China Sea. Paper SPE 180685 Presented at the IADC/SPE Asia Pacific Drilling Technology Conference, Singapore, 22-24 August, 2016.

Vryzas, Z., Kelessidis, V. C., Nalbantian, L. et al. Effect of temperature on the rheological properties of neat aqueous Wyoming sodium bentonite dispersions. Applied Clay Science, 2017, 136: 26-36.

Wang, F., Tan, X., Wang, R., et al. High temperature and high pressure rheological properties of high-density water-based drilling fluids for deep wells. Petroleum Science, 2012, 9(3): 354-362.

Xu, Z., Song, X., Li, G., et al. Development of a transient non-isothermal two-phase flow model for gas kick simulation in HTHP deep well drilling. Applied Thermal Engineering, 2018, 141: 1055-1069.

Zhang, J., Lu, Y., Chen, Y., et al. Effect of temperature recovery on time-dependent wellbore stability in geothermal drilling. Paper ARMA-CUPB 19-4482 Presented at the ARMA-CUPB Geothermal International Conference, Beijing, China, 5-8 August, 2019.

Zhang, Z., Xiong, Y., Pu, H., et al. Effect of the variations of thermophysical properties of drilling fluids with temperature on wellbore temperature calculation during drilling. Energy, 2021, 214: 119055.